Geomechanics and Engineering, *Vol. 22, No. 1 (2020) 25-33*
DOI: https://doi.org/10.12989/gae.2020.22.1.025

Incorporating ground motion effects into Sasaki and Tamura prediction equations of liquefaction-induced uplift of underground structures

Jui-Ching Chou[1] and Der-Guey Lin*[2]

[1]Department of Civil Engineering, National Chung Hsing University, 145 Xingda Rd., South Dist., Taichung 40227, Taiwan, R.O.C.
[2]Department of Soil and Water Conservation, National Chung Hsing University, 145 Xingda Rd., South Dist., Taichung 40227, Taiwan, R.O.C.

(Received January 30, 2020, Revised May 13, 2020, Accepted May 18, 2020)

Abstract. In metropolitan areas, the quantity and density of the underground structure increase rapidly in recent years. Even though most damage incidents of the underground structure were minor, there were still few incidents causing a great loss in lives and economy. Therefore, the safety evaluation of the underground structure becomes an important issue in the disaster prevention plan. Liquefaction induced uplift is one important factor damaging the underground structure. In order to perform a preliminary evaluation on the safety of the underground structure, simplified prediction equations were introduced to provide a first order estimation of the liquefaction induced uplift. From previous studies, the input motion is a major factor affecting the magnitude of the uplift. However, effects of the input motion were not studied and included in these equations in an appropriate and rational manner. In this article, a numerical simulation approach (FLAC program with UBCSAND model) is adopted to study effects of the input motion on the uplift. Numerical results show that the uplift and the Arias Intensity (Ia) are closely related. A simple modification procedure to include the input motion effects in the Sasaki and Tamura prediction equation is proposed in this article for engineering practices.

Keywords: uplift; underground structure; liquefaction; FLAC; ground motion

1. Introduction

In the modern society, because of the need of housing, infrastructures and many other constructions in urban areas, the quantity and density of the underground structure (e.g., lifelines and tunnels) increase rapidly. Most of damage incidents of the underground structure may only have a small impact on people’s daily life. There were still few incidents causing a great loss in lives and economy in the past (e.g., the fatal explosion in Kaohsiung City, Southern Taiwan in 2014 caused by the leakage of flammable fluid pipelines). As a consequence, more attentions should be paid to the evaluation of the stability and safety of the underground structure system.

Soil liquefaction is one crucial hazard affecting the stability and the integrity of the underground structure. When the soil liquefies, the underground structure could be damaged by the uplift caused by the buoyancy force and the movement of the liquefied soil surrounding the structure. Model tests and numerical simulations were performed to explore the uplift mechanisms and factors (soil properties, structure properties, seismic loadings) affecting the uplift (Koseki *et al.* 1997, Sasaki and Tamura 2004 Liu and Song 2005, Chou 2010, Chou *et al.* 2011, Tobita *et al.* 2011, Chian and Madabhushi 2012a, b, Kang *et al.* 2013, Madabhushi and Madabhushi 2015, Han and Liu 2016, Watanabe *et al.* 2016 and Bao *et al.* 2017, Castiglia *et al.* 2018). Conclusions from previous studies categorized the uplift mechanisms as: (1) Ratcheting (Sand flow), (2) Pore water migration and (3) Heave of the soil underneath the underground structure. In addition, past studies (Sasaki and Tamura 2004, Liu and Song 2005, Chou 2010, Madabhushi and Madabhushi 2015 and Bao *et al.* 2017) indicated that the input motion characteristics (input motion duration and amplitude) have significant influences on the magnitude of the uplift.

In order to perform a preliminary and fast evaluation on the safety of the underground structure system, several simplified prediction equations (Sasaki and Tamura, 2004; Tobita *et al.* 2011 and Kang *et al.* 2014) were introduced to estimate the liquefaction induced uplift. Effects of the input motion characteristics were included in these equations but not in an appropriate and rational way.

In this article, a numerical simulation approach using finite difference method (FDM) program, FLAC program (version 7), with UBCSAND model, a constitutive model for soil liquefaction modeling, is adopted to study effects of the input motion characteristics on the uplift. Then, a simple approach incorporating the input motion effects into the Sasaki and Tamura prediction equation is proposed.

2. Simplified prediction equations

Sasaki and Tamura (2004) conducted a series of centrifuge model tests to study effects of different factors (thickness of the liquefiable layer underneath structure,

*Corresponding author, Professor
E-mail: dglin@nchu.edu.tw

http://www.techno-press.org/?journal=gae&subpage=7
ISSN: 2005-307X (Print), 2092-6219 (Online)

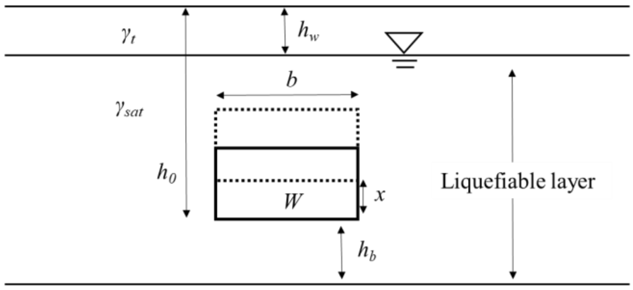

Fig. 1 Calculation model and variables for the simplified equation (modified from Sasaki and Tamura 2004)

geometry of the underground structure, relative density of the liquefiable soil etc…) on the underground structure uplift induced by liquefaction and proposed a simplified prediction equation to estimate the liquefaction-induced uplift of the underground structure. The equation of Sasaki and Tamura (2004) can be considered as a robust uplift prediction equation because the equation incorporates important factors affecting the uplift and most equation input variables can be obtained from general soil properties (e.g., SPT-N value, unit weight). Therefore, in this study, the Sasaki and Tamura equation is selected for a further modification. In Sasaki and Tamura (2004), the uplift of the underground structure, x, is expressed as:

$$x = \left[1 - exp\left(-\frac{\gamma_{sat} b}{C} t\right)\right] \times \{[\gamma_t h_w + \gamma_{sat}(h_0 - h_w)]b - W\} \Big/ \gamma_{sat} b \tag{1}$$

where γ_t is the unit weight of the soil above the water table, γ_{sat} is the saturated unit weight of the soil, W is the weight of the structure and the overburden soil, h_w is the depth of the water table, h_0 is the depth of the bottom of the structure, b is the width of the structure, t is time (the duration of the soil liquefied during the shaking), C is the resistance coefficient. The resistance coefficient can be expressed as:

$$c[t/ms] = 50000 \times b[m] \times (b/h_b + 1) \times \left(\frac{\sigma_h' - \sigma_v'}{2\sigma_h'}\right)^{0.5} \times R \times {F_L}^{1.5} \tag{2}$$

where h_b is the thickness of liquefiable layer underneath the structure, σ_h' is the effective overburden stress of the surrounding soil at depth to bottom of structure, σ_v' is the effective overburden stress at depth to bottom of structure, R is the cyclic shear resistance ratio estimated from the design specifications for highway bridges in Japan (2001), F_L (= R/L) is the liquefaction resistance factor in the same design specifications and L is the seismic shear stress ratio. The calculation procedure of the design specifications for highway bridges in Japan (2001) is same with JRA (1996). The detailed calculation procedures were explained and discussed in Tamura (2014).

The calculation model and the associated variables are shown in Fig. 1. In Sasaki and Tamura (2004), the input motion effects on the uplift were included via L and t. However, these two variables are not able to fully capture the input motion effects on the uplift which results in an overestimated uplift for cases subjected to the real earthquake motions (Sasaki and Tamura 2004).

3. Numerical model calibration

Several constitutive models were built to model behaviors of the soil liquefaction and coded with FEM or FDM programs, such as FINN model (Martin *et al.* 1975 and Byrne 1991), UBCSAND model (Puebla *et al.* 1997 and Beaty and Byrne 1998) and PM4sand model (Boulanger and Ziotopoulou 2013, Ziotopoulou and Boulanger 2013, 2016).

In this study, FLAC program (FDM program) with UBCSAND model is adopted for the numerical simulation. The large deformation of the soil induced by the soil liquefaction can be capture easily via the large strain mode in FLAC program which cannot be easily captured by other numerical tools. The UBCSAND model (Puebla *et al.* 1997 and Beaty and Byrne 1998) is a simple elastoplastic stress/strain model for sand to simulate the liquefaction phenomenon. In addition, the UBCSAND model has been coded with FLAC program and validated by applications to centrifuge model tests, laboratory element tests, and field measurements from real earthquakes (Puebla *et al.* 1997, Beaty and Byrne 1998 and Yang *et al.* 2004). Chou *et al.* (2010) validated the capability of FLAC program with UBCSAND model to simulate the uplift mechanisms of the underground structure by comparing with centrifuge test results. Ardeshiri-Lajimi *et al.* (2016) and Dashti and Bray (2014) also had promising results using UBCSAND model to study and explore responses of a shallow foundation structure during the soil liquefaction. Therefore, adopting FLAC with UBCSAND model as the numerical simulation tool in this study is feasible and reasonable. In this study, input parameters of UBCSAND model are first calibrated using the centrifuge test results from Sasaki and Tamura (2004). Subsequently, different types of input motions (earthquake motions and sinusoidal motions) are applied to the calibrated model to study input motion effects on the underground structure.

In Sasaki and Tamura (2004), the dimensions of the centrifuge model and the underground structure in prototype scale are 40 m × 10 m (length × height) and 5 m × 3.75 m (length × height) as shown in Fig. 2. The centrifuge model has one layer of Toyoura sand (Dr = 50 %) and was subjected to a sinusoidal wave (20 cycles and 1.2 Hz). Time histories of 6 instruments (DV1, P2, PM2, PU1, A0, A2, AM2 shown in Fig. 2) are selected for

Table 1 Uplifts from numerical simulation cases and centrifuge tests (Sasaki and Tamura 2004)

Centrifuge test No	Relative Density (Dr)	Input Motion	Centrifuge test Uplift	Simulation Uplift
CASE 97-06	30%	Sinusoidal motion of 20 cycles and 1.2 Hz. Ia = 13.14 m/s	1.24 m	1.22 m
CASE 98-01	50%		1.09 m	1.04 m
CASE 97-02	80%		0.23 m	0.23 m

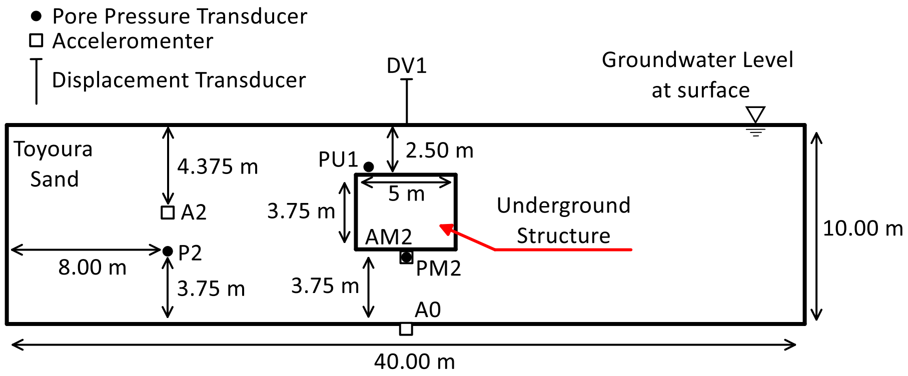

(a) Centrifuge test model and instruments (modified from Sasaki and Tamura 2004)

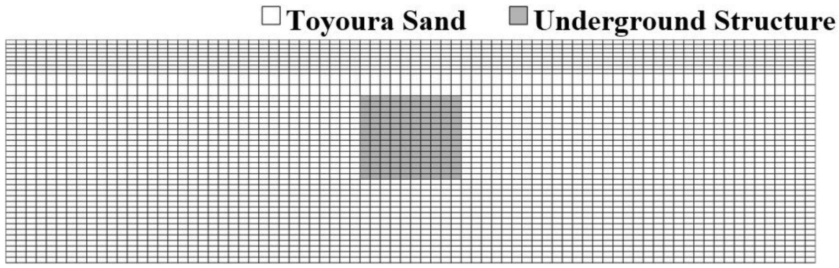

(b) Finite difference mesh of numerical model

Fig. 2 Geometric model of centrifuge test and the numerical simulation model

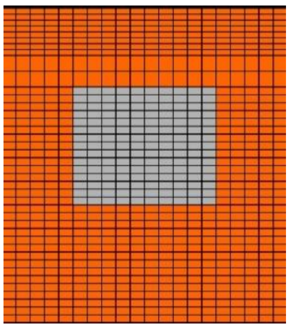

(a) Original Mesh

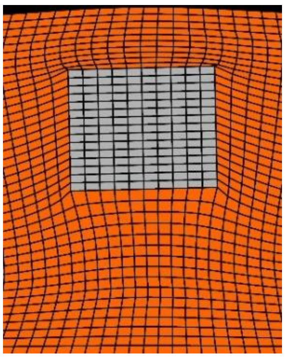

(b) Deformed Mesh

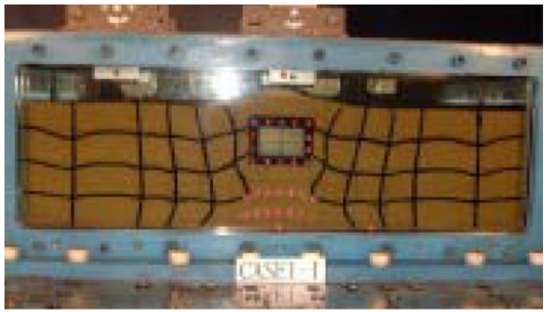

(c) Deformed Centrifuge Model (Sasaki and Tamura 2004)

Fig. 3 Deformation patterns of the numerical simulation model and the centrifuge test model

comparisons. In the numerical simulation, the underground structure is modeled using the elastic model with a large shear modulus and bulk modulus (about 4-5 times of the maximum elastic moduli of Toyoura sand) and the Toyoura sand is modeled using the UBCSAND model. The detailed descriptions and formulations of the UBCSAND model inputs are discussed in Beaty and Byrne (2011).

Numerical simulation results of *D*r = 50% case are compared with CASE98-01 in Sasaki and Tamura (2004) as shown in Figs. 3 and 4. The deformed shape of the FLAC model is similar to the deformed shape of the centrifuge test. The sand surrounding the underground structure moves underneath the underground structure and lifts the underground structure which is one of the uplift mechanisms (Ratcheting or Sand flow) observed in Chou *et al.* (2010) and Koseki *et al.* (1997). Measurements of instruments from FLAC simulation are slightly larger than those from the centrifuge test. However, the trends of monitoring data are similar. Comparisons show that the calibrated numerical model can be used for further analyses. The uplift of the underground structure at different relative density cases are listed in Table 1. The uplift of the numerical simulation and of the centrifuge test are not identical but their differences are less than 2%. The calibrated input parameters are listed in Table 2.

4. Numerical simulation results

Earthquake motions used in the numerical simulation consist of 48 time histories (2 horizontal directions of 24 strong motion stations) from 5 disastrous earthquake events in Taiwan (Chi-Chi Earthquake in 1999, Chiayi Earthquake in 1999, Chiashien Earthquake in 2010, Tainan Earthquake in 2016 and Hualian Earthquake in 2018).

In order to incorporate effects of the magnitude and

Table 2 Calibrated input parameters of the UBCSAND model

Underground Structure			
Unit weight of Underground Structure	0.80 t/m^3	Sasaki and Tamura (2004)	
UBCSAND Model Inputs of Toyoura sand (Beaty and Byrne, 2011and Sasaki and Tamura, 2004)			
Relative Density of Toyoura sand (Dr)	30%	50%	80%
Unit weight of Saturated Toyoura Sand	1.88 t/m^3	1.92 t/m^3	1.98 t/m^3
Elastic shear modulus (G^e) number, $K_{GE}{}^*$	600	1000	1400
Elastic shear exponent, $n_e{}^*$	0.5	0.5	0.5
Elastic bulk modulus (B^e) number, $K_B{}^*$	600	1000	1400
Elastic bulk exponent, $m_e{}^*$	0.5	0.5	0.5
Plastic shear modulus (G^p) number, $K_{GP}{}^{**}$	40	100	200
Plastic shear exponent, $n_p{}^*$	0.5	0.5	0.5
Critical state friction angle, $\phi_{Cs}{}^*$	33.0°	33.0°	33.0°
Peak friction angle, $\phi_{Peak}{}^*$	33.4°	34.2°	39.0°
Failure ratio, $R_f{}^{**}$	0.92	0.90	0.70

*Estimated using equations suggested in Beaty and Byrne (2011). These equations are function of $(N_1)_{60}$. In this study, $(N_1)_{60} = C_d \times Dr^2$ and $C_d = 46$

**K_{GP} and R_f are adjusted to fit the centrifuge test results

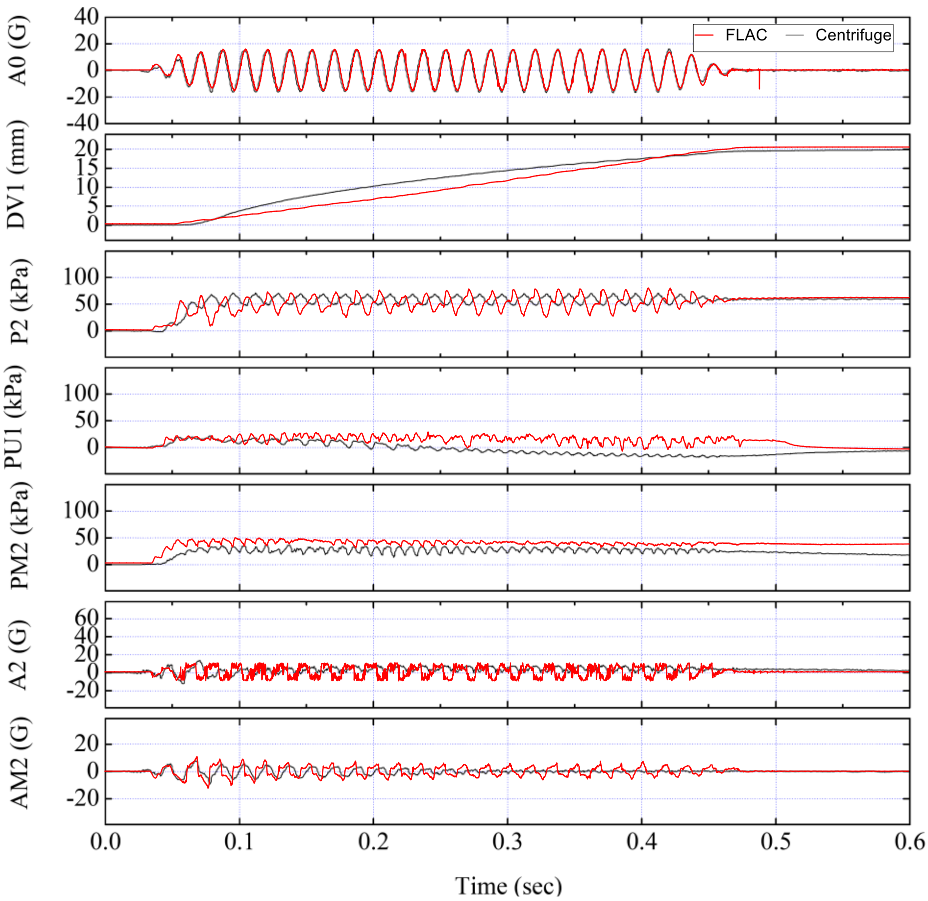

Fig. 4 Time histories of selected measurements of the centrifuge test and the FLAC simulation (modified from Sasaki and Tamura 2004)

distance into the content of the earthquake motion, selected time histories possess M_w = 5.8 ~ 7.6, Distance = 2 km ~ 40 km and PGA = 0.10 g ~ 0.65 g (shown in Fig. 5). For the comparison purpose, all time histories are scaled to the same peak acceleration when they are applied to the numerical model.

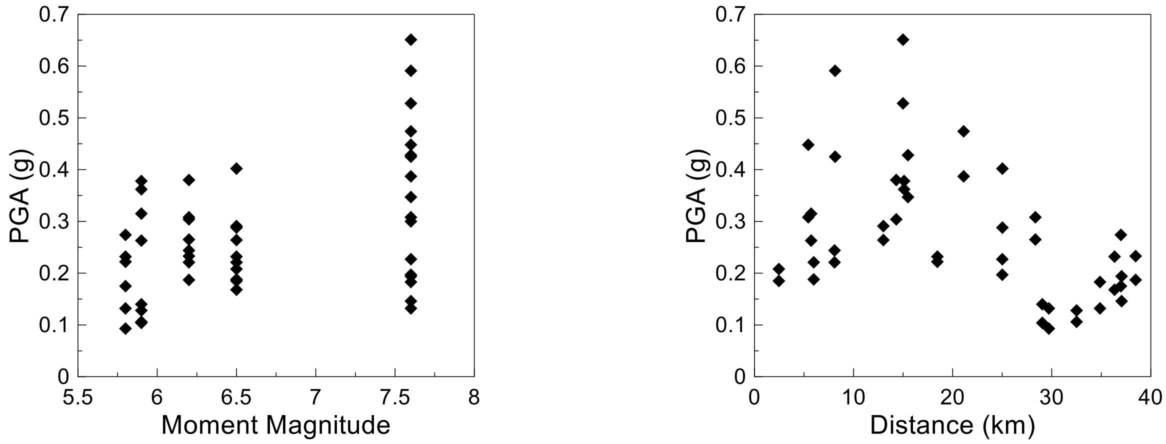

Fig. 5 Distributions of peak ground acceleration, magnitude and distance of selected earthquake motions

Table 3 Cases adopted in the numerical simulation

Soil Relative Density (D_r)	Peak Acceleration of Input Motion	Total Simulation Cases
30 %, 50 % and 80 %	0.1 g	17*
	0.2 g	49**
	0.3 g	50***
	0.4 g	50***

*The 0.1 g cases were not performed for *D*r = 80 %. 17 cases = 16 earthquake motions from Chi-Chi Earthquake + 1 sinusoidal motion of 20 cycles and 1.2 Hz.

**49 cases of 0.2 g = 48 earthquake motions + 1 sinusoidal motion of 20 cycles and 1.2 Hz.

***50 cases of 0.3 g and 0.4 g = 48 earthquake motions + 1 sinusoidal motion of 20 cycles and 1.2 Hz + 1 extended sinusoidal motion of 30 cycles and 1.2 Hz.

Information of numerical simulation cases are listed in Table 3. Three relative densities (*D*r = 30%, 50% and 80%) are selected to study responses from loose to dense sand and peak accelerations of input motions are scaled to four levels (0.1 g, 0.2 g, 0.3 g and 0.4 g). Other than earthquake motion cases, sinusoidal motion cases used in the centrifuge test are also included.

Uplifts of cases with *D*r = 50% and peak acceleration = 0.3 g were correlated to several indices (peak input acceleration, peak input velocity, peak input displacement and Arias Intensity) representing characteristics of an input motion (shown in Fig. 6). Comparing the data scattering and the index availability, the Arias Intensity (*Ia*), which represents the energy or the strength of a motion, is the optimal index to correlate with the uplift.

In order to cover a representative range of *Ia* value, an appropriate range of *Ia* (shown in Fig. 7) is estimated using the *Ia* prediction equation (within 1 standard deviation) from TNGA project (Taiwan's Next Generation Attenuation Relationship for Ground Motion Project, Sinotech, 2012) with *D*r = 30% ~ 80% (convert to shear wave velocity), M_w = 6.0 ~ 7.6 and peak input acceleration = 0.1 g ~ 0.4 g. Nevertheless, for peak input acceleration = 0.3 g and 0.4 g, values of *Ia* do not situate within the proposed range of *Ia*. Consequently, two extended sinusoidal motions (extended from 20 to 30 cycles) are added in 0.3 g and 0.4 g simulation cases (*Ia* = 19.02 m/s for 0.3 g and 33.67 m/s for 0.4 g) to meet the upper limit of the proposed range of *Ia* ranges.

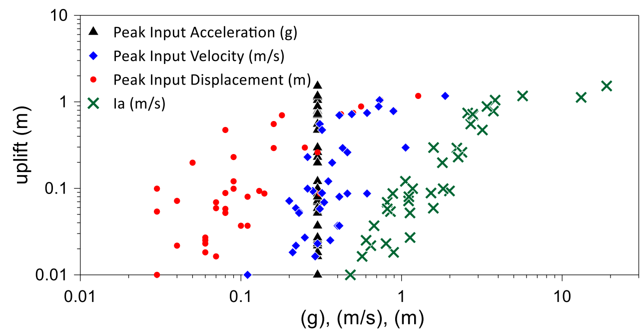

Fig. 6 Correlation of uplifts with earthquake motion indices for *D*r = 50% and peak input acceleration = 0.3 g

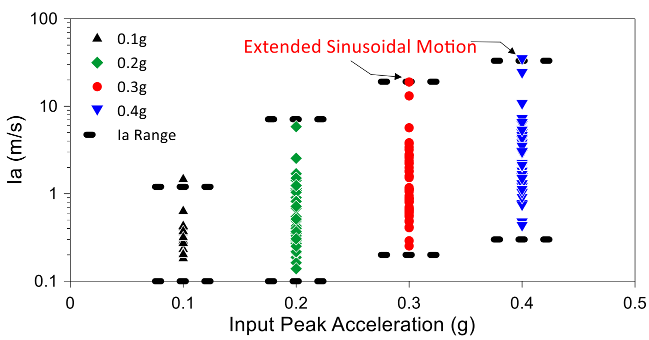

Fig. 7 Distribution of *Ia* values for input motions used in simulations

Simulation results from different *D*r and peak input

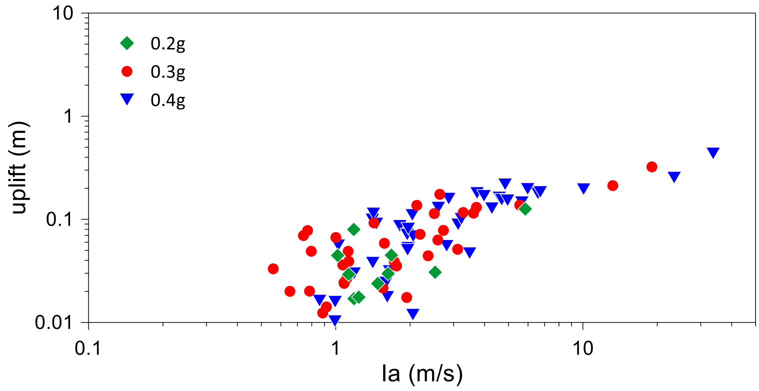

(a) *Dr* =80%

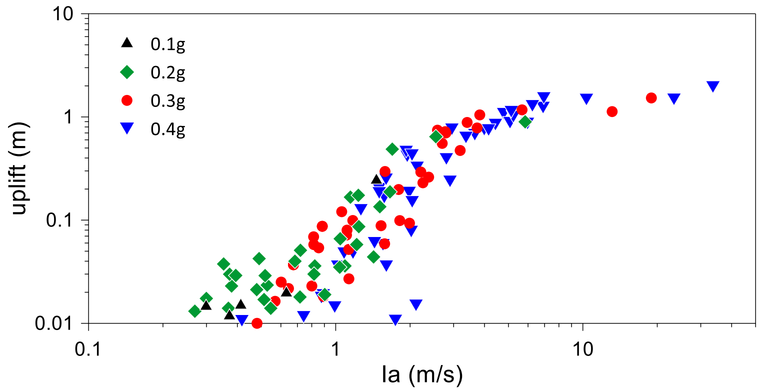

(b) *Dr* =50%

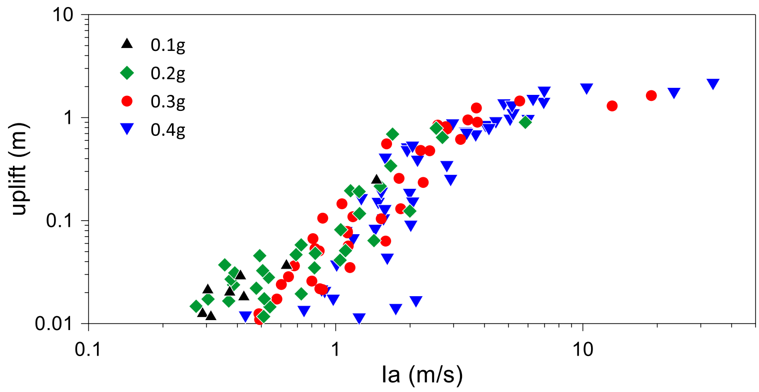

(c) *Dr* =30%

Fig. 8 Correlation of uplifts with Arias intensity (*Ia*) for different relative densities of soil

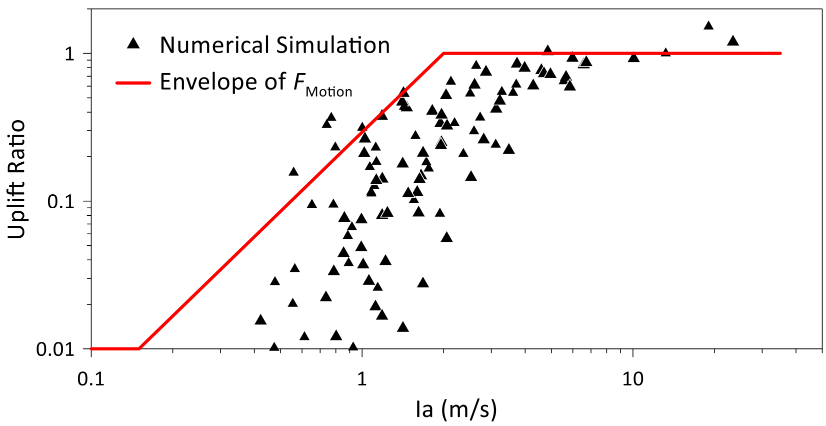

(a) *Dr* =80%

Fig. 9 Uplift Ratios and envelopes of F_{motion} with *Ia*

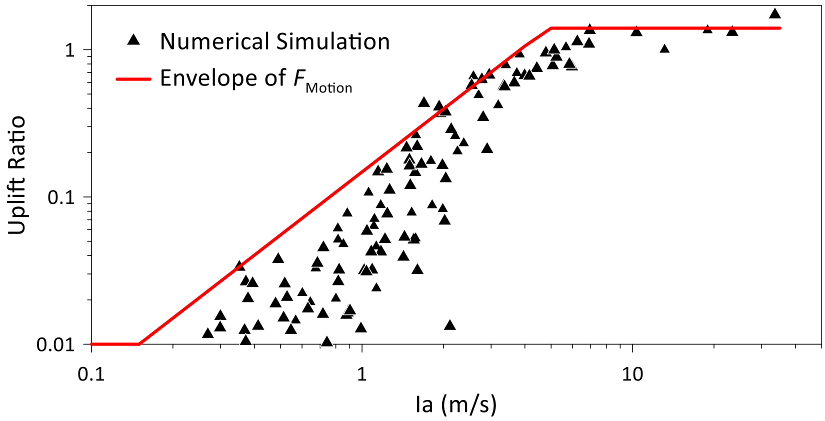

(b) *Dr* =50%

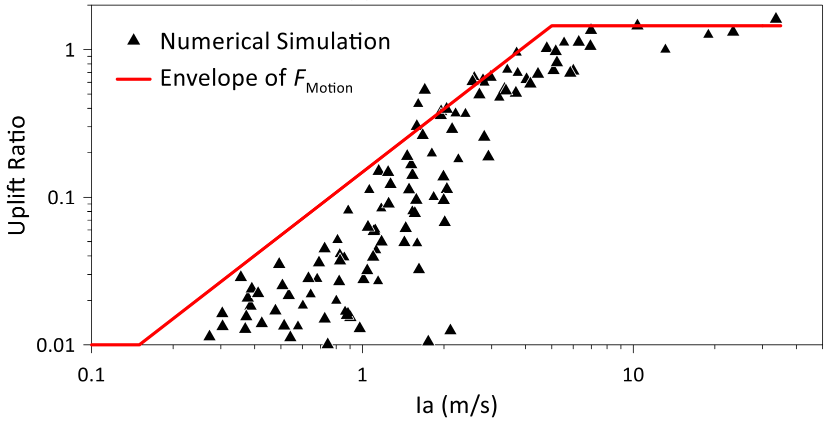

(c) *Dr* =30%

Fig. 9 Continued

accelerations are shown in Fig. 8. Several trends are observed: (1) uplift and *Ia* have exhibit an approximately linear relationship under the log-log scale; (2) data become more scattered when uplift is less than 0.1 m; (3) under a specific *Dr* condition, not the peak input acceleration but the *Ia* value controls the uplift magnitude; (4) there exists an upper limit of the uplift for each *Dr* condition.

5. Numerical simulation results

The input motion effects on the uplift were included in the prediction equation of Sasaki and Tamura (2004) via two variables, L ($F_L = R/L$) and t. The variable L is the seismic shear stress ratio which is a function of the peak acceleration of the input motion and the variable t is the duration of the soil liquefied during shaking. As shown in Fig. 6 and Fig. 8, although the simulation cases with identical peak input accelerations, they could also generate a wide range of the uplift. In addition, because of the irregularity of the earthquake motion, it is difficult to estimate t value appropriately. These explain why the uplift prediction shows a good agreement with uplifts from sinusoidal motion cases (easy to estimate t value) but overestimates for real earthquake cases in Sasaki and Tamura (2004). In this study, a modification of the uplift prediction equation incorporating the input motion effects is proposed to estimate the modified uplift, Up_{mod}:

Table 4 Variables of F_{Motion} Equation

Dr (%)	30	50	80
Slope	1.42	1.42	1.78
F_{max}	1.45	1.40	1.00

when *Dr* falls between values in this table, variables can be estimated using linear interpolation

$$Up_{mod} = F_{Motion} \times Up_{ref} \tag{3}$$

where F_{Motion} is a factor derived from the uplift ratio curve (shown in Fig. 9) to account for the input motion effects, Up_{ref} is a reference uplift. The uplift ratio in Fig. 9 is calculated as the uplift divided by the uplift of the sinusoidal motion case (cases listed in Table 3) with the same *Dr* value. To simplify the calculation and obtain a conservative prediction, the upper bound envelope of the uplift ratio is used for F_{Motion}:

$$\begin{gathered} F_{Motion} = e^{\{[\ln(Ia)-\ln(0.15)]\times Slope\}} \\ 0.01 \le F_{Motion} \le F_{max} \end{gathered} \tag{4}$$

where *Ia* is the Arias Intensity of the input motion. *Slope* is the gradient of the uplift ratio envelope and F_{max} is the maximum value of F_{Motion} (listed in Table 4). In addition, when the *Ia* value is less than 0.15 m/s (shown in Fig. 8), the uplift becomes smaller than 0.01 m. In practice, this amount of uplift can be considered having no effect on the safety of the underground structure. However, for the conservative purpose, the minimum value of F_{Motion} is specified as 0.01 when the *Ia* value is less than 0.15 m/s (see Fig. 9). Up_{ref} is calculated using Eqs. (1) and (2) with t = 30 seconds and L estimated from peak input acceleration = 0.3 g which is corresponding to the sinusoidal motion case used in the uplift ratio calculation.

6. Discussions

The uplift ratio data in Fig. 9 indicate that the prediction of Sasaki and Tamura (2004) (*Ia* = 13.14 m/s and Uplift Ratio = 1.0) overestimates the uplift in low *Ia* cases (which have uplift ratios less than 1.0) and underestimates the uplift in high *Ia* cases (which have uplift ratios greater than 1.0). Therefore, it is not appropriate to estimate the uplift using the original equation in Sasaki and Tamura (2004). The proposed modified equation provides an alternative method to implement a relatively accurate and conservative uplift prediction of the underground structure.

When modeling in the large strain mode of FLAC program, a "bad geometry" error message is sent out and the simulation is terminated when the geometry of an element is distorted to a certain extent. In order to continue the simulation, geometries of the "bad geometry" element and surrounding elements need to be adjusted. In this study, several high uplift cases (uplift > 1.2 m) encountered the "bad geometry" issue and the geometry adjustment was made to continue the simulation. Because the geometry adjustment alters the stress and the strain distributions of adjusted elements, the adjustment could affect the deformation pattern of high uplift cases which is used to define the values of $F_{\max}$. Therefore, it is suggested to perform physical model tests (e.g., centrifuge tests) to verify the suitability of $F_{\max}$ listed in Table 3. The centrifuge tests can also be used to validate the proposed F_{motion} curves.

R variable (the cyclic shear resistance ratio) in Equation (2) is estimated using procedures of the design specifications for highway bridges in Japan. In other countries or areas, different procedures (Seed *et al.* 1985; Youd *et al.* 2001; Tokimatsu and Yoshimi, 1983; AIJ, 2001) are also used to estimate the cyclic shear resistance ratio. To enhance the applicability of the modified Sasaki and Tamura prediction equation, it is beneficial to include the cyclic shear resistance ratio from different methods.

7. Conclusions

The stability of the underground structure system in the modern society becomes increasingly important because the damage of the system could lead to a devastating disaster and cause an enormous loss in lives and economy. The liquefaction induced uplift is one major cause jeopardizing the safety of the underground structure system. Simplified prediction equations were introduced to obtain a first order estimation of the liquefaction induced uplift in the past. However, effects of the input motion on the uplift were not considered appropriately in these equations.

In this study, a numerical approach (FLAC program with UBCSAND model) is adopted to study effects of the input motion on the uplift. Numerical results reveal that the uplift is proportional to the Arias Intensity (*Ia*) of the input motion. A simple procedure is proposed to modify the prediction equation of Sasaki and Tamura (2004) which overestimates the uplift in low *Ia* cases and underestimates in high *Ia* cases. In the modified equation, the modified uplift, Up_{mod}, is equivalent to the multiplication of two variables ($Up_{\mathrm{mod}} = F_{\mathrm{Motion}} \times Up_{\mathrm{ref}}$): (1) F_{Motion}, a normalized factor (a function of *Ia* value) to account for the input motion effects, and (2) Up_{ref}, a reference uplift of the underground structure estimated using the equation of Sasaki and Tamura (2004) under the specific conditions. This modification procedure is simple and easy to use because all inputs can be obtained from standard procedures and equations straightforwardly. The modified equation can provide a relatively accurate and conservative estimation of the liquefaction induced uplift of the underground structure for a preliminary safety evaluation.

Acknowledgments

This research is funded by the Office of Research and Development of National Chung-Hsing University (NCHU) and Ministry of Science and Technology, Taiwan, R.O.C. under Grant no. MOST 107-2218-E-005-020-MY2. I also like to thank the National Center for Research on Earthquake Engineering (NCREE) for providing the catalog of earthquake motions.

References

Architectural Institute of Japan (AIJ), (2001), *Recommendations for Design of Building Foundations* (in Japanese).

Ardeshiri-Lajimi, S., Yazdani, M. and Assadi-Langroudi, A. (2016), "A Study on the liquefaction risk in seismic design of foundations", *Geomech. Eng.*, **11**(6), 805-820. http://doi.org/10.12989/gae.2016.11.6.805.

Bao, X., Xia, Z., Ye, G., Fu, Y. and Su, D. (2017), "Numerical analysis on the seismic behavior of a large metro subway tunnel in liquefiable ground", *Tunn. Undergr. Sp. Technol.*, **66**, 91-106. http://doi.org/10.1016/j.tust.2017.04.005.

Beaty, M. and Byrne, P. M. (1998), "An effective stress model for predicting liquefaction behaviour of sand", *Geotech. Earthq. Eng. Soil Dyn.*, **75**(1), 766-777.

Boulanger, R.W. and Ziotopoulou, K. (2013), "Formulation of a sand plasticity plane-strain model for earthquake engineering applications", *Soil Dyn. Earthq. Eng.*, **53**, 254-267. http://doi.org/10.1016/j.soildyn.2013.07.006.

Byrne P.M. (1991), "A cyclic shear-volume coupling and pore-pressure model for sand", *Proceedings of Second International Conference on Recent Advances in Geotechnical Earthquake Engineering and Soil Dynamics*, St. Louis, Missouri, U.S.A.

Castiglia, M., de Magistris, F.S. and Napolitano, A. (2018), "Stability of onshore pipelines in liquefied soils: Overview of computational methods", *Geomech. Eng.*, **14**(4), 355-366. http://doi.org/10.1016/B978-0-12-397949-0.00004-2.

Chian, S.C. and Madabhushi, S.P.G. (2012a), "Effect of buried depth and diameter on uplift of underground structures in liquefied soils", *Soil Dyn. Earthq. Eng.*, **41**, 181-190.

http://doi.org/10.1016/j.soildyn.2012.05.020.
Chian, S.C. and Madabhushi, S.P.G. (2012b), "Effect of soil conditions on uplift of underground structures in liquefied soil", *J. Earthq. Tsunami*. **6**(4), 1250020. http://doi.org/10.1142/S1793431112500200.
Chou, J.C. (2010), "Centrifuge modeling of the BART transbay tube and numerical simulation of tunnels in liquefying ground", Ph.D. Dissertation, University of California, Davis, California, U.S.A.
Chou, J.C., Kutter, B.L., Travasarou, T. and Chacko, J.M. (2011), "Centrifuge modeling of seismically induced uplift for the BART transbay tube", *J. Geotech. Geoenviron. Eng.*, **137**(8), 754-765. http://doi.org/10.1061/(ASCE)GT.1943-5606.0000489.
Han, Y. and Liu, H. (2016), "Failure of circular tunnel in saturated soil subjected to internal blast loading", *Geomech. Eng.*, **11**(3), 421-438. http://doi.org/10.12989/gae.2016.11.3.421.
Itasca Consulting Group Inc, (2011), *FLAC Version 7.0*, Software, https://www.itascacg.com/software/flac.
Japan Road Association (JRA), (1996), *Design Specifications for Highway Bridges*, *Part V Seismic Design*, Japan (in Japanese).
Kang, G.C., Tobita, T. and Iai, S. (2014), "Seismic simulation of liquefaction-induced uplift behavior of a hollow cylinder structure buried in shallow ground", *Soil Dyn. Earthq. Eng.*, **64**, 85-94. http://doi.org/10.1016/j.soildyn.2014.05.006.
Kang, G.C., Tobita, T., Iai, S. and Ge, L. (2013), "Centrifuge modeling and mitigation of manhole uplift due to liquefaction", *J. Geotech. Geoenviron. Eng.*, **139**(3), 458-469. http://doi.org/10.1061/(ASCE)GT.1943-5606.0000769.
Koseki, J., Matsuo, O. and Koga, Y. (1997), "Uplift behavior of underground structures caused by liquefaction of surrounding soil during earthquake", *Soils Found.*, **37**(1), 97-108. http://doi.org/10.3208/sandf.37.97.
Liu, H. and Song, E. (2005), "Seismic response of large underground structures in liquefiable soils subjected to horizontal and vertical earthquake excitations", *Comput. Geotech.*, **32**(4), 223-244. http://doi.org/10.1016/j.compgeo.2005.02.002.
Madabhushi, S.S.C. and Madabhushi, S.P.G. (2015), "Finite element analysis of floatation of rectangular tunnels following earthquake induced liquefaction", *Indian Geotech. J.*, **45**(3), 233-242. http://doi.org/10.1007/s40098-014-0133-3.
Martin, G.R., Finn, W.D.L. and Seed, H.B. (1975), "Fundamentals of liquefaction under cyclic loading", *J. Geotech. Div.*, **101**(GT5), 423-438.
Puebla, H., Byrne, P.M. and Phillips, R. (1997), "Analysis of CANLEX liquefaction embankments: Prototype and centrifuge models", *Can. Geotech. J.*, **34**(5), 641-657. http://doi.org/10.1139/t97-034.
Sasaki, T. and Tamura, K. (2004), "Prediction of liquefaction-induced uplift displacement of underground structures", *Proceedings of the 36th Joint Meeting US-Japan Panel on Wind and Seismic Effects*.
Seed, H.B., Tokimatsu, K., Harder, L.F. and Chung, R.M. (1985), "The influence of SPT procedures in soil liquefaction resistance evaluation", *J. Geotech. Eng. Div.*, **111**(12), 1425-1445. http://doi.org/10.1061/(ASCE) 0733-9410(1985)111:12(1425).
Sinotech Engineering Consultants (Sinotech) (2012), *Taiwan's Next Generation Attenuation Relationship for Ground Motion Project Report*, Taipei, Taiwan (in Chinese).
Tamura, K. (2014), "Seismic design of highway bridge foundations with the effects of liquefaction since the 1995 Kobe earthquake", *Soils Found.*, **54**(4), 874-882. https://doi.org/10.1016/j.sandf.2014.06.017.
Tobita, T., Kang, G.C. and Iai, S. (2011), "Centrifuge modeling on manhole uplift in a liquefied trench", *Soils Found.*, **51**(6), 1091-1102. http://doi.org/10.3208/sandf.51.1091.
Tokimatsu, K. and Yoshimi, Y. (1983), "Empirical correlation of soil liquefaction based on SPT N-value and fines content", *Soils Found.*, **23**(4), 56-74. http://doi.org/10.3208/sandf1972.23.4_56.
Watanabe, K., Sawada, R. and Koseki, J. (2016), "Uplift mechanism of open-cut tunnel in liquefied ground and simplified method to evaluate the stability against uplifting", *Soils Found.*, **56**(3), 412-426. http://doi.org/10.1016/j.sandf.2016.04.008.
Yang, D., Naesgaard, E., Byrne, P.M., Adalier, K. and Abdoun, T. (2004), "Numerical model verification and calibration of George Massey Tunnel using centrifuge models", *Can. Geotech. J.*, **41**(5), 921-942. http://doi.org/10.1139/t04-039.
Youd, T.L., Idriss, I.M., Andrus, R.D., Arango, I., Castro, G., Christian, J.T., Dobry, R., Finn, W.D.L., Harder, L.F., Hynes, M.E., Ishihara, K., Koester, J.P., Liao, S.C.C., Marcuson, III., W.F., Martin, G.R., Mitchell, J.K., Moriwaki, Y., Power, M.S., Robertson, P.K., Seed, R.B. and Stokoe, II, K.H. (2001), "Liquefaction resistance of soils: Summary report from the 1996 NCEER and 1998 NCEER/NSF Workshops on evaluation of liquefaction resistance of soils", *J. Geotech. Geoenviron. Eng.*, **127**(10), 817-833. http://doi.org/10.1061/(ASCE)1090-0241(2001)127:10(817).
Ziotopoulou, K. and Boulanger, R.W. (2013), "Calibration and implementation of a sand plasticity plane-strain model for earthquake engineering applications", *Soil Dyn. Earthq. Eng.*, **53**, 268-280. http://doi.org/10.1016/j.soildyn.2013.07.009.
Ziotopoulou, K. and Boulanger, R.W. (2016), "Plasticity modeling of liquefaction effects under sloping ground and irregular cyclic loading conditions", *Soil Dyn. Earthq. Eng.*, **84**, 269-283, http://doi.org/10.1016/j.soildyn.2016.02.013.

CC